In Vitro/In Vivo Correlation for Drug-Drug Interactions

Jan Wahlstrom and Larry Wienkers

Contents

Introduction 2

Methods and Assumptions 3
Brief Primer on In Vitro Enzyme Kinetics 3
Types of DDIs 4
Experimental Considerations in Vitro 9
Prediction of DDI for the Clinical Situation 12
Quantitative Prediction of Clinical DDIs 12
Regulatory Guidance and DDIs 13
Additional Considerations 16
Is Concern over Plasma Protein Displacement DDIs Justified? 17
Impact of Pharmacogenetics on DDIs 17

Conclusion 18

References and Further Reading 18

Abstract

Characterizing the potential for drug-drug interactions is critical to underwriting patient safety as new chemical entities proceed through the drug discovery and development pipeline. In vitro experiments to characterize the type and extent of interaction have been developed to inform chemical modifications early in discovery and to estimate the magnitude of potential interactions as drugs progress into the clinic. Regulatory guidance provides flow schemes based on a comprehensive understanding of drug disposition to enable decision-making as to whether particular clinical interaction studies need to be run and, if so, how they may be designed. Integration of information from in vitro, in vivo, and clinical sources provides the basis for drug labeling and the safe administration of drugs post-launch.

J. Wahlstrom
Amgen, Inc, Pharmacokinetics and Drug Metabolism, Thousand Oaks, CA, USA
e-mail: janw@amgen.com

L. Wienkers (✉)
Amgen, Inc, Pharmacokinetics and Drug Metabolism, South San Francisco, CA, USA
e-mail: wienkers@amgen.com

F.J. Hock, M.R. Gralinski (eds.), *Drug Discovery and Evaluation: Methods in Clinical Pharmacology*,
https://doi.org/10.1007/978-3-319-56637-5_14-1

Introduction

Drug-drug interactions (DDIs) occur when the dosing of a drug influences the pharmacokinetics (PK) or pharmacodynamics (PD) of a second drug. It has been estimated that 1–5% of hospital admissions may be due to DDIs (Day et al. 2017). Drugs such as mibefradil, terfenadine, and nefazodone (QTc prolongation) or bromfenac, alosetron, and cerivastatin (toxicity) have been removed from the market due to a high potential for DDIs (Wienkers and Heath 2005). Drug labels may contain a black box warning if concern over DDI potential is great enough. Factors influencing the likelihood and severity of DDIs may include age (the very young and aged are more susceptible), disease state, genetics, and polypharmacy, where the risk of DDIs increases dramatically when a patient is taking four or more medications simultaneously (Jacubeit et al. 1990). Due to the importance of DDIs in the drug discovery and development process, the US Food and Drug Administration (in vitro and clinical FDA Guidance for Industry 2017a,b) and the European Medicines Agency (EMA Guideline on the investigation of drug interactions 2012) have released and continually update regulatory guidance on the design and performance of in vitro and clinical DDI studies, as well as decision trees to guide decision-making as to whether particular DDI studies may be necessary as a new molecular entity (NME) proceeds through the drug discovery and development pipeline.

As shown in Fig. 1, co-administration of a second drug to a drug dosed to steady state may increase or decrease the drug concentration of the first drug. Both the direction and magnitude of the DDI effect are important (Rowland and Martin 1973). Reduced drug concentrations, due to a process called induction, may fall below the efficacious threshold leading to loss of pharmacological effect. Increased drug concentrations, due to enzyme inhibition or inactivation, may exceed a toxicological threshold leading to adverse events. The range of drug concentrations and doses between the efficacious and toxicological threshold is called the therapeutic index. Drugs with a narrow therapeutic index are of high concern for

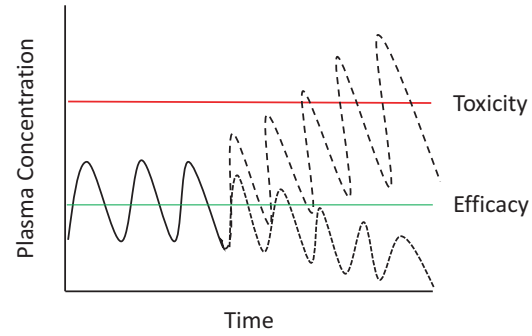

Fig. 1 Effects of inhibition or induction on a victim drug

DDIs, as small increases or decreases (less than two-fold) in drug concentration or doses may result in loss of efficacy or adverse drug reactions, respectively (Levy 1998). Drugs with a wide therapeutic index may exhibit large magnitude of DDIs without significant pharmacological or toxicological effect. The affected drug is called the victim, object, or substrate, whereas the affecting drug is called the perpetrator, precipitant, or inhibitor.

DDIs may be PK or PD based. PK is the study of what the body does to a drug. Typically, plasma or serum concentrations of a drug are measured as a surrogate for the concentration of drug at the site of pharmacological activity. This information is then visualized as a plasma concentration-time profile and quantified with PK parameters such as the area under the plasma concentration-time curve (AUC) or the maximum observed concentration of drug (C_{max}) as determinants of overall drug exposure. PK-based drug interactions typically involve the inhibition or inactivation of enzyme activity, or the enhancement of enzyme expression, leading increases or decreases in drug exposure, respectively. PK-based DDIs also include phenomena such as loss of exposure due to increased gastrointestinal pH observed upon co-administration with an acid-reducing agent (Chung et al. 2015). PD is the effect of a drug on the body. PD-based DDIs occur when drugs influence each other's pharmacological effects directly, such as the co-administration of two sedatives to potentiate activity.

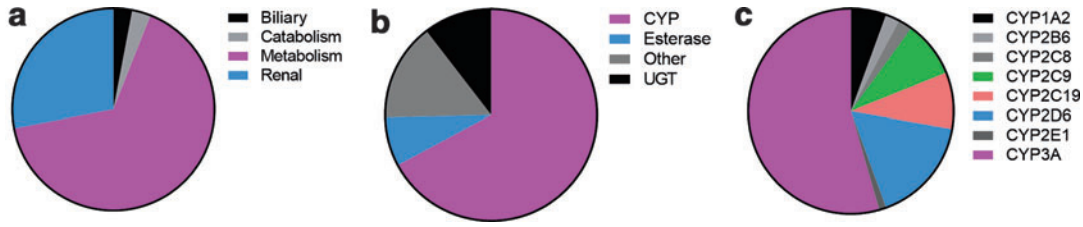

Fig. 2 Clearance mechanisms for the top 200 drugs of 2016

Small-molecule drugs are typically cleared through a combination of metabolism, renal excretion, and biliary excretion (Lin and Lu 1997). Those drugs undergoing metabolism may be cleared through phase I oxidation by enzymes such as the cytochrome P450s (CYPs), flavin monooxygenases (FMO), or aldehyde oxidase (AO). They may undergo phase II conjugation by enzymes such as the uridine 5′-diphosphoglucuronosyltransferase (UGTs), sulfotransferases (SULTs), or N-acetyltransferases (NATs). Drugs may also be cleared through transport by enzymes such as p-glycoprotein (P-gp), breast cancer resistance protein (BCRP), or the organic-peptide-transporting polypeptides (OATPs). Protein-based therapeutics, such as antibodies, have other routes of clearance such as catabolism. The relative contribution of clearance mechanisms for the 200 most prescribed drugs of 2016 is listed in Fig. 2a, where metabolism is the primary mechanism of clearance, followed by renal excretion. Of those drugs undergoing metabolism, approximately 70% are cleared by CYPs (Fig. 2b). The CYP3A enzymes are responsible for approximately 55% of the CYP-mediated metabolism (Fig. 2c). Thus, the CYPs, and particularly CYP3A, are the primary enzymes responsible for the metabolism of many of the highly prescribed drugs of 2016.

Methods and Assumptions

Brief Primer on In Vitro Enzyme Kinetics

A typical approach to characterizing enzyme kinetics in vitro is to examine product formation at multiple substrate concentrations. The results are then visualized in graph of substrate concentration versus reaction velocity (ν). Under Michaelis-Menten conditions, it is assumed that the enzyme (E), substrate (S), and enzyme-substrate complex (ES) are in rapid equilibrium and that product (P) formation is irreversible to give the following reaction scheme (Michaelis and Menten 1913).

$$E + S \leftrightarrow ES \rightarrow E + P$$

Mathematical representation of Michaelis-Menten kinetics provides the following equation:

$$\nu = \frac{(V_{\max}{}^{*}[S])}{(K_m + [S])} \quad (1)$$

where ν is the reaction velocity, $V_{\max}$ is the maximal reaction velocity, $[S]$ is the substrate concentration, and K_m is the substrate concentration at half-maximal velocity. Visualization (graph of ν versus $[S]$) of in vitro data under Michaelis-Menten conditions produces a hyperbolic curve (Fig. 3a) and a straight line in an Eadie-Hofstee visualization (Frere et al. 1983) of $\nu/[S]$ versus ν (Fig. 3e).

Atypical (non-Michaelis-Menten) kinetic profiles may be observed for some drug-metabolizing enzymes (DMEs). For experiments where substrate alone is present, apparent autoactivation or biphasic or substrate inhibition kinetics may be observed (Hutzler and Tracy 2002). It has been proposed that atypical kinetic phenomena occur because two or more substrates are present in the DME active site at the same time (Korzekwa et al. 1998). Atypical kinetics is more likely observed for DMEs with a large active site such as CYP2C9 and CYP3A4. Autoactivation occurs when a

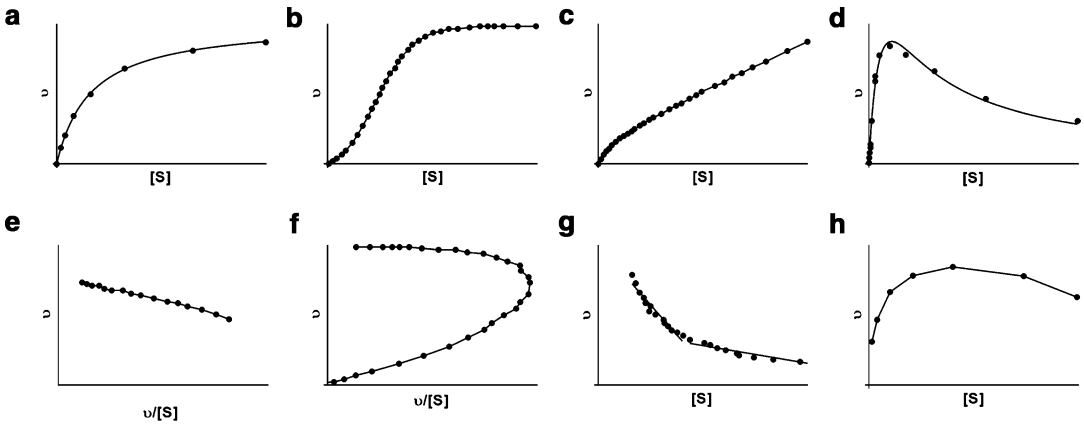

Fig. 3 Velocity versus substrate and Eadie-Hofstee graphs for hyperbolic kinetics (**a**, **e**), sigmoidal kinetics (**b**, **f**), biphasic kinetics (**c**, **g**), and apparent substrate inhibition kinetics (**d**, **h**)

substrate enhances its own metabolism as the substrate concentration increases. Autoactivation results in a sigmoidal visualization of ν versus $[S]$. Autoactivation often begins to occur at low substrate concentrations and may be difficult to observe in the ν versus $[S]$ visualization (Fig. 3b); a hook in the Eadie-Hofstee plot is a more readily observed diagnostic for the presence of autoactivation (Fig. 3f). The Hill equation may be used to estimate kinetic parameters:

$$\nu = \frac{V_{\max}{}^{*}[S]^{n}}{S_{50}{}^{n} + [S]^{n}} \tag{2}$$

where n is an exponent that indicates how far the observed kinetics are deviating from a standard value of 1 and S_{50} is the substrate concentration at which half-maximal reaction velocity has been achieved.

Biphasic conditions occur when enzyme architecture allows for both a low and a high affinity site for metabolism on the same enzyme for a single substrate; the reaction rate does not saturate and instead proceeds linearly as substrate concentrations are increased. Biphasic kinetic data may be modeled using the following equation (Kumar et al. 2006a):

$$\nu = \frac{(V_{\max 1}{}^{*}[S]) + \left(CL_{\text{int}}{}^{*}[S]^{2}\right)}{(K_{m1} + [S])} \tag{3}$$

where K_{m1} and $V_{\max 1}$ are the kinetic parameters for the high affinity contribution to the enzyme reaction and CL_{int} is used to represent the intrinsic clearance of the linear portion of the kinetics (Fig. 3c). Two distinct contributions to turnover are readily visible in the Eadie-Hofstee plot for this type of kinetics (Fig. 3g). Biphasic kinetics may also be observed in multienzyme systems when two or more enzymes are responsible for the turnover of a substrate that exhibit different K_m estimates.

Substrate inhibition kinetics occur when increasing substrate concentrations causes a decrease in product formation (Fig. 3d). Eadie-Hofstee visualization of this type of kinetics exhibits decreasing ν as $\nu/[S]$ increases (Fig. 3h) and may be represented by the equation (Lin et al. 2001):

$$\nu = \frac{V_{\max}}{1 + \dfrac{K_m}{[S]} + \dfrac{[S]}{K_i}} \tag{4}$$

where K_i represents the binding of the substrate to the inhibitory site.

Types of DDIs

There are three primary mechanisms of PK-based drug-drug interactions: reversible inhibition,

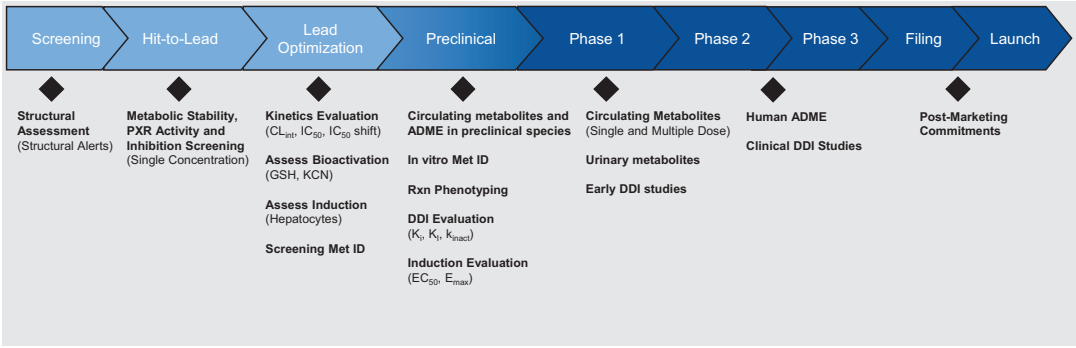

Fig. 4 Key drug information to enable characterization of DDI risk

time-dependent inhibition, and induction (Wahlstrom et al. 2006). Reversible inhibitors interact with an enzyme's architecture through non-covalent bonding, which may occur within or external to the enzyme active site. Time-dependent inhibitors are characterized by a change in observed inhibition potency over time, most often caused by metabolism-mediated enzyme inhibition (such as formation of an inhibitory metabolite) or inactivation. The primary concern with enzyme inhibition or inactivation is an increase in victim drug levels to a point where adverse effects may begin to occur. Induction occurs due to increases in protein expression levels generally caused by an increase in gene transcription. In contrast to inhibition, induction reduces victim drug levels, where the primary concern is loss of efficacy. Characterization of the potential for inhibition and induction occur throughout the drug discovery and development process, where initial single concentration screening experiments are followed up using higher content experiments that may be used to predict DDI effects in the clinical situation. A typical paradigm for information gathering relevant to predicting clinical DDIs is shown in Fig. 4. The higher content experiments include the IC_{50} estimation, where the effects of multiple concentrations of inhibitor are determined relative to a single concentration of substrate (at K_m); the K_i (inhibitory constant) estimation, where multiple substrate and inhibitor concentrations are tested to fully characterize the type of inhibition observed; and the EC_{50} and E_{max} experiment for induction, where multiple inducer concentrations are tested to determine their maximal effect of induction (E_{max}) and the inducer concentration at half-maximal induction (EC_{50}). In addition to direct DDI characterization, an understanding of the mechanism(s) of clearance, the enzymes responsible for metabolism, the presence of metabolites (particularly circulating metabolites), and likely administered co-medications based on therapeutic area are key pieces of information to underwrite the potential risk of DDIs.

Reversible inhibition may be further differentiated by types, which include competitive inhibition, noncompetitive inhibition, uncompetitive inhibition, mixed inhibition, and atypical or multisite inhibition. A summary of inhibition kinetic characteristics is shown in Table 1. Competitive inhibitors compete with a substrate for binding to enzyme, where enzyme binding of the substrate or inhibitor is mutually exclusive. This competition is often for the enzyme active site. The presence of a competitive inhibitor raises the apparent K_m for the substrate, as increased substrate concentration is needed to outcompete the inhibitor for the active site. Nonlinear fitting of in vitro data (Eq. 5 for competitive inhibition) is now com-

Table 1 Inhibition types and characterization

Inhibition type	Inhibition characteristics	Apparent effects	Lineweaver-Burk (1/[S] vs. 1/ν)
Competitive	S and I compete for E binding	$K_m\uparrow$, $V_{max}\leftrightarrow$	Intersect on y axis
Noncompetitive	I binding alters E architecture, reducing activity	$K_m\leftrightarrow$, $V_{max}\downarrow$	Intersect on x axis
Uncompetitive	I binds only to the ES complex	$K_m\downarrow$, $V_{max}\downarrow$	Parallel lines
Mixed	I binds to E and ES	$K_m\downarrow$ or $\uparrow$, $V_{max}\downarrow$	Intersect with $x < 0$ and $y > 0$
Multisite or atypical	Multiple ES complexes possible	Situational	NA

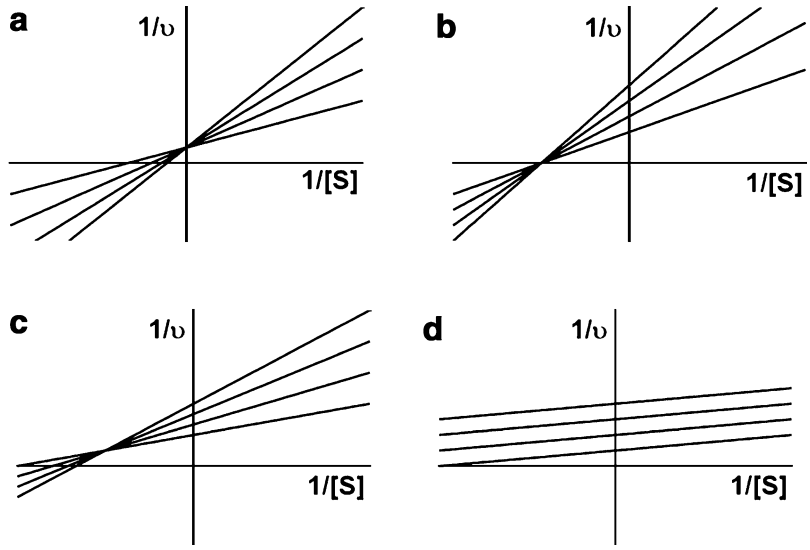

Fig. 5 Lineweaver-Burk plots for competitive (**a**), noncompetitive (**b**), mixed (**c**), and uncompetitive inhibition (**d**)

monly used to estimate inhibition potency and assess inhibition mechanism; [I] is the concentration of the inhibitor in the equations. A Lineweaver-Burk visualization (graph of 1/[S] versus 1/ν, Fig. 5a) aids in determining inhibition type, as linear regression of the inhibition data at each substrate concentration will intersect at a common point on the y-axis of the visualization (Lineweaver and Burk 1934).

$$v = \frac{V_{max} \bullet [S]}{K_m\left(1 + \frac{[I]}{K_i}\right) + [S]} \tag{5}$$

Noncompetitive inhibition, in contrast, results when an inhibitor has equal affinity for the enzyme, regardless of whether or not substrate is bound, but reduces enzyme activity, typically through allosteric alteration of the enzyme architecture. Inhibition potency for noncompetitive inhibition may be determined using Eq. 6. In a Lineweaver-Burk visualization, linear regression of the inhibition data at each substrate concentration characteristically intersects on the x-axis (Fig. 5b).

$$v = \frac{V_{max} \bullet [S]}{K_m\left(1 + \frac{[I]}{K_i}\right) + [S]\left(1 + \frac{[I]}{K_i}\right)} \tag{6}$$

Uncompetitive inhibition occurs when the inhibitor binds only the enzyme-substrate (ES) complex and not the enzyme itself. True uncompetitive inhibition is rarely observed in practice. Inhibition potency for an uncompetitive inhibitor may be estimated using Eq. 7.

Lineweaver-Burk visualization results in diagnostic parallel lines that are parallel and do not intersect (Fig. 5c).

$$v = \frac{V_{\max} \bullet [S]}{K_m + [S]\left(1 + \frac{[I]}{K_i}\right)} \tag{7}$$

Mixed inhibition occurs when the inhibitor binds to the enzyme and the ES complex, but the binding is stronger to one of the reaction constituents. Inhibition potency may be estimated through nonlinear regression of Eq. 8. A Lineweaver-Burk representation of mixed inhibition has the intersection of linear regression lines in the upper left quadrant of the graph as a characteristic (Fig. 5d).

$$v = \frac{V_{\max} \bullet [S]}{K_m\left(1 + \frac{[I]}{K_i}\right) + [S]\left(1 + \frac{[I]}{K_i'}\right)} \tag{8}$$

Analogous to the observations with substrates, enzymes with large or flexible active sites may exhibit atypical or two-site inhibition profiles, where the substrate and the inhibitor occupy the enzyme active site simultaneously. This simultaneous occupancy of the active site may result in partial inhibition, where an inhibitor incompletely inhibits the turnover of a substrate, even as the inhibitor level is increased. Two-site models may also be applied to in vitro inhibition data where fitting of competitive, noncompetitive, uncompetitive, and mixed inhibition models to observed data is poor. Two-site inhibition is one potential explanation for substrate-dependent inhibition, where the same inhibitor exhibits different apparent inhibition potency for the same enzyme when compared using different substrates (VandenBrink et al. 2012).

Time-dependent inhibition (TDI) refers to a general increase in inhibition potency over time. TDI may be caused by slow binding or access of the inhibitor to the enzyme or other, more common mechanisms including metabolism-dependent inhibition (MDI) or mechanism-based inactivation (MBI). MDI includes the formation of inhibitory or inactivating metabolites that are metabolism-dependent. MBI is characterized by irreversible or quasi-irreversible enzyme inactivation, which include mechanisms such as heme destruction, heme alkylation, metabolite intermediate complex (MIC) formation, or heme alkylation (Foti et al. 2011). Experiments to determine the mechanism of MBI and the corresponding diagnostic results for CYPs are outlined in Table 2. Seven criteria have been proposed by Silvermann to characterize a drug as a MBI, including time dependence, saturation of inactivation at high inactivator concentrations, protection of inactivation by the presence of substrate, irreversibility, 1:1 stoichiometry of inactivator to enzyme, and metabolism dependence; the inactivation must also occur before the reactive species exits the active site (Silverman 1995). A parameter used to characterize the efficiency of inactivation is the partition ratio, which is the sum of all metabolic events divided by the number of inactivation events (Kunze and Trager 1993). A low partition ratio indicates very efficient inactivation of an enzyme.

TDI may be assessed in vitro through the use of a preincubation, where an aliquot of preincubate is added to initiate the probe substrate reaction after a predetermined period of time. For the single point experiment, activity loss is determined by the following equation:

$$\%\text{Loss} = 100 \bullet \left[\left(\frac{\text{Activity}_{\text{inactivator}}}{\text{Activity}_{\text{control}}}\right)_{\text{NoCofactor}} - \left(\frac{\text{Activity}_{\text{inactivator}}}{\text{Activity}_{\text{control}}}\right)_{\text{WithCofactor}}\right] \tag{9}$$

An IC_{50} shift experiment takes advantage of preparations needed for a reversible IC_{50} experiment but adds additional information through a preincubation step. The IC_{50} shift output (Fig. 6a) indicates TDI by a left shift in potency for the preincubated samples. For the high content TDI experiment, multiple concentrations of inhibitor and multiple time points are used to characterize TDI activity. The acquired data is transformed to natural log (ln) and linear regression of the loss of activity over time at each TDI concentration is calculated (Fig. 6b) to obtain the observed, pseudo-first-order rate constant of inactivation

Table 2 Mechanisms of CYP inactivation with diagnostic experiments

Inactivation mechanism	Loss of activity	Loss of CO binding	Loss of native heme	Other diagnostics	Prototypical example
Apoprotein adduction	Yes	Possibly	No	Formation of GSH, cysteine, lysine, or cyanide adducts	Raloxifene (CYP3A4)
Heme destruction	Yes	Yes	Yes	NA	Mibefradil (CYP3A4)
Heme adduction	Yes	Possibly	Yes	NA	Gemfibrozil glucuronide (CYP2C8)
MIC formation	Yes	Yes	No	Appearance of peak at 440–450 nm (UV–vis spectrum); $Fe(CN)_6$ restores activity	Verapamil (CYP3A4)

(k_{obs}). If the time-dependent inhibition is saturable with increasing concentrations of inhibitor, kinetics parameters can be estimated with an equation that is an analog of that used to obtain Michaelis-Menten kinetic parameters (Eq. 10, Fig. 6c):

$$k_{obs} = \frac{(k_{inact}{}^{*}[I])}{(K_I + [I])} \tag{10}$$

where k_{inact} is the maximal rate of inactivation and K_I is the inhibitor concentration at half-maximal inhibition.

Enzyme induction typically involves an increase in enzyme transcription (Lin 2006). For DMEs, the process often involves ligand binding to one of three nuclear receptors: the aryl hydrocarbon receptor (AHR), the constitutive androstane receptor (CAR), or the pregnane X receptor (PXR). CAR and PXR are primarily expressed in the gut and liver, sites that are co-localized with high expression levels of DMEs. PXR is the receptor of main concern, as it is a major transcriptional regulator of CYP3A4 and P-gp protein expression. Enzyme induction is a time-dependent process thought to involve ligand binding to the receptor and translocation of the bound receptor to the cell nucleus, where binding to DNA sequences in the promoter region causes the recruitment of coactivators, thus increasing protein transcription rates and the quantity of active enzyme available for drug metabolism. Early screening typically involves cell lines engineered to encode the PXR-binding domain. Interaction with PXR ligands activates the receptor, leading to an increase in luciferase production that may be used as a surrogate for functional PXR activity. The gold standards for characterizing DME induction are experiments using human hepatocytes. Increases in mRNA levels for individual DMEs are used to determine a maximal response (E_{max}), as well as the inducer concentration required for half-maximal activity (EC_{50}) using the following equation:

$$\text{Effect} = \frac{(E_{max}{}^{*}[\text{Inducer}])}{(EC_{50} + [\text{Inducer}])} \tag{11}$$

These parameters may be used to quantitatively estimate induction potential in the clinical situation. As the induction assay requires fully functional hepatocytes, a commonly encountered confounding factor in the determination of induction parameters is cell toxicity; toxicity is commonly observed with increasing concentration for cytotoxic drugs and may prevent full characterization of induction potential.

The presence of inflammatory cytokines may lead to a process called downregulation, which has the opposite effect of induction. Downregulation is most commonly seen with inflammatory diseases, where IL-6 and other cytokines may lead to an apparent reduction in transcription and expression of DMEs, reducing the turnover of DME substrates and leading to higher drug levels (Evers et al. 2013). Treatment of the inflammatory disease may reduce cytokine-mediated influence on DMEs, leading to increased transcription, protein synthesis, and DME turnover, leading to

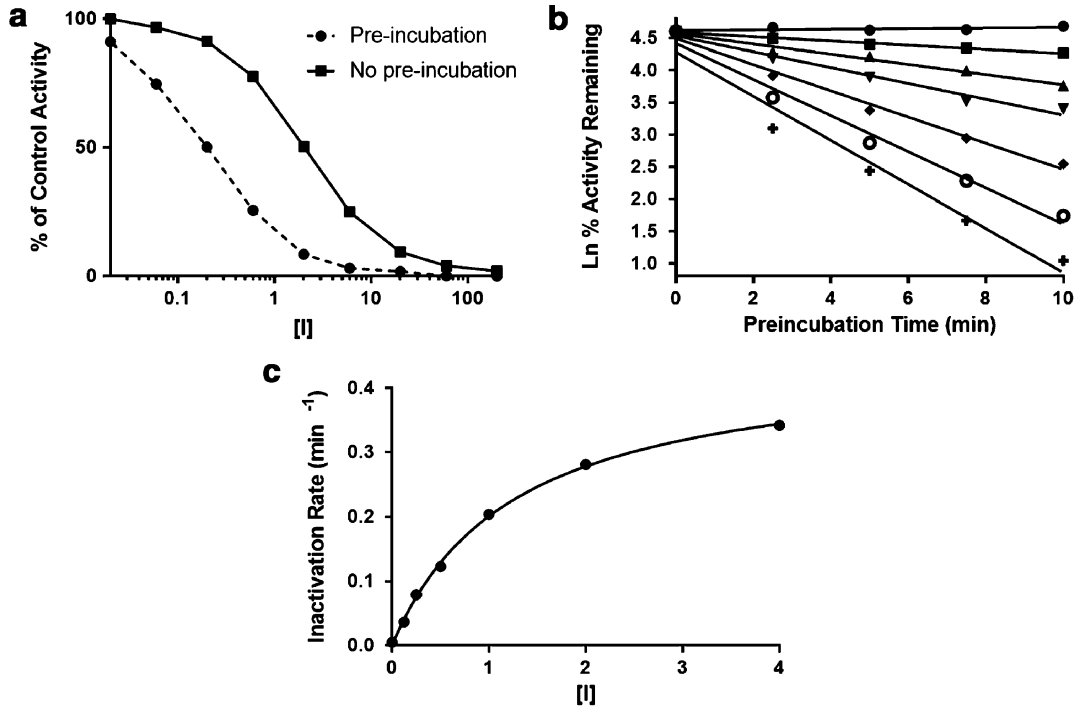

Fig. 6 Representative TDI experiments: IC50 shift (**a**), percent activity remaining (**b**), and K_I, k_{inact} (**c**)

lower drug levels. Due to the complexities in the downregulation process, neither in vitro nor preclinical models may serve as predictors of the clinical situation with the current state of knowledge (Dickmann et al. 2011).

Experimental Considerations in Vitro

Both the FDA and EMA DDI Guidance provide details on the design of in vitro experiments informing DDI studies. A major factor in assessing the fraction of metabolism (f_m) of an NCE (DDI potential as a victim) and in designing reversible in vitro inhibition experiments (DDI potential as a perpetrator) is selecting the appropriate enzyme source. Different sources of enzymes for in vitro experiments include subcellular fractions such as human liver microsomes, S9 or cytosolic liver fractions, recombinant enzymes, hepatocytes, or organ slices. Each of these in vitro systems contains a different compliment of DMEs and requires specific incubation conditions for optimal activity. Centrifugation of liver tissue homogenate produces three subcellular fractions: microsomes, which are isolated from the cell pellet after centrifugation; S9 fractions, which are the soluble enzyme constituents after centrifugation; and cytosolic fractions, which are obtained from the supernatant after resuspension of the pellet and a second centrifugation. Due to ease of use and availability of pooled lots across a large number of donors, human liver microsomes are often selected as the relevant in vitro source of enzyme to determine inhibition potency for membrane-bound DMEs that reside in the endoplasmic reticulum, such as the CYPs, FMOs, and UGTs. Relevant cofactors, such as the reduced form of nicotinamide adenine dinucleotide phosphate (NADPH) or uridine 5′-diphosphoglucuronic acid (UDPGA) for CYPs/FMOs or UGTs, respectively, must be added to microsomal incubations to initiate and sustain enzyme activity. Additives, such as the pore-forming agent, alamethicin, are added to overcome latency of the UGTs to observe in vitro activity. Other additives, such as

magnesium chloride, are often added to microsomal preparations to help stabilize CYP structure to support maximal activity. Liver S9 fractions contain soluble DME constituents, which may be appropriate for examining the effect of inhibitors on soluble enzymes such as aldehyde oxidase (AO), epoxide hydrolase (EH), sulfotransferases (SULTs), or carboxylesterases (CES); S9 preparations may contain some residual CYP content as well. Cytosolic fractions contain soluble enzymes such as AO and the SULTs. Recombinant, expressed enzymes are often used to aid in determining which DMEs are involved in the metabolism of an NCE; they are less commonly used to determine inhibition potency, as the expression systems are artificial (typically expressed in a baculovirus vector), tend to overexpress enzyme relative to liver fractions, and may lack protein-protein interactions that exist in subcellular liver fractions. Hepatocytes contain the full complement of DMEs and the prerequisite cofactors for DME activity but are more difficult to prepare and use. The preparation of liver or other organ slices is technically challenging, which is why they are rarely used. Integration of the in vitro metabolism data in its entirety allows for initial assessment of f_m; regulatory guidance recommends follow-up for instances where greater than 25% of DME metabolism is believed to proceed by a single metabolism pathway (Fig. 7).

The Pharmaceutical Research and Manufacturers of America (PhRMA) have published an overview on the conduct of in vitro DDI studies (Bjornsson et al. 2003). Key factors identified in experimental design are reaction conditions including solvent effects, protein concentration, nonspecific binding to the incubation matrix, and probe substrate selection. The manuscript recommends screening initial reaction conditions so that the enzymatic reactions are linear with regard to both time and protein concentration. Low protein levels minimize inhibitor depletion in the incubations and reduce the impact of nonspecific binding to the incubation matrix. Measurement of the unbound drug fraction in the incubation matrix is often used to correct in vitro measurements for the prediction of clinical DDIs and therefore is a useful parameter to measure in vitro. Low organic solvent concentrations, particularly of DMSO, are used to minimize possible effects on DME activity. The PhRMA publication outlines the use of selective probe substrate reactions to assess inhibitory potential for individual DMEs. A list of commonly used selective probe substrates and inhibitors for CYP-mediated DDI are shown in Table 3. The FDA and EMA DDI Guidance are updated on a regular basis and provide another source for commonly used probe substrates. Due to its large active site and the potential for atypical kinetics, two probe substrates are recommended to assess inhibitory potency for CYP3A4 from both an FDA and EMA perspective (specifically midazolam and testosterone based on current EMA DDI Guidance). For situations where large differences in inhibition potency are observed between the two probes, the most potent inhibition should be used for prediction of clinical DDIs (Foti et al. 2010).

PhRMA has also published an overview on the conduct and design of experiments to characterize TDI (Grimm et al. 2009). For TDI experiments, the additional experimental factors of concern are protein concentration in the preincubation, preincubation time, incubation time, dilution factor, and concentrations of the inactivator and probe substrate. Protein concentration in the preincubation is important because a balance of turnover versus nonspecific binding is desired; increasing protein will not necessarily translate to an increase in turnover or inactivation rate. Preincubation time is important, as it is generally desired to use initial rates for the inactivation calculations; too little or too much inactivation may increase the difficulty in calculating these kinetic parameters. For IC_{50} shift experiments, dilution from a preincubation is not done, so that the substrate concentration remains the same (at k_m) for the incubations with and without preincubation. Dilution is normally carried out for the K_i and k_{inact} experiment, as it is desired to minimize the potential for reversible inhibition; the dilution also reduces the potential for inactivation during the probe substrate reaction. High substrate concentrations are used (often five- to tenfold of k_m), to ensure that sufficient substrate is present to

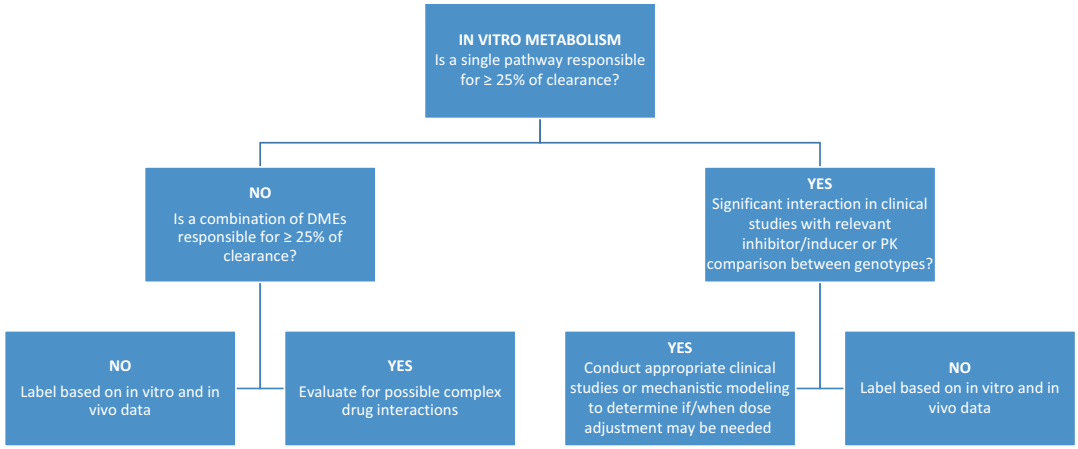

Fig. 7 Decision tree to determine victim DDI potential

Table 3 Typical CYP-selective probe substrates, inhibitors, and inactivators

CYP isoform	Substrate	K_m (μM)	Inhibitor	K_i (μM)	Inactivator	K_I (μM)	K_{inact} (min^{-1})
1A2	Phenacetin	20	α-Napthoflavone	0.016	Furafylline	4.4	0.14
2B6	Bupropion	50	Clotrimazole	0.022	Ticlopidine	0.32	0.43
2C8	Paclitaxel	5	Montelukast	0.004	Gemfibrozil glucuronide	35	0.022
2C9	Diclofenac	4	Sulfaphenazole	0.041	Tienilic acid	1.0	0.17
2C19	(S)-Mephenytoin	20	(+)-N-Benzylnirvanol	0.027	Ticlopidine	5.3	0.077
2D6	Dextromethorphan	4	Quinidine	0.012	Paroxetine	1.1	0.11
2E1	Chlorzoxazone	50	Diethyldithiocarbamate	16	Disulfiram	12	0.02
3A4/5	Midazolam	2	Ketoconazole	0.002	Mifepristone	3.6	0.079
3A4/5	Testosterone	20	Ketoconazole	0.005	Mifepristone	3.6	0.079

outcompete remaining inactivator from the enzyme active site.

For in vitro induction experiments, key features identified by PhRMA include the exposure time of the hepatocytes to the NME, the concentrations of the NME used, the potential of the NME to cause cellular toxicity, and the experimental output to measure (Chu et al. 2009). Regulatory guidance from EMA and FDA both recommend the use of three or more hepatocyte donors; the hepatocytes may be cryopreserved or fresh. Changes in mRNA levels versus positive controls are the assay readout for development studies; DME activity may be assessed in some cases as a secondary endpoint. Regulatory guidance from EMA guidance recommends exposure to test article over 72 h. Both FDA and EMA guidance recommend refreshing exposure to the NME daily; EMA recommends measuring the amount of parent drug from the incubation at several times on the final day of the experiment. Single concentrations of NME may be used to characterize induction potential in the discovery environment, while multiple NME concentrations are used to characterize EC_{50} and E_{max} for the development environment. EMA guidance recommends in vitro concentrations exceeding 50-fold the mean unbound C_{max} value for DMEs present in the liver, with in vitro concentrations of NME exceeding 0.1*dose/250 mL as an estimate for DMEs present in the gut (CYP3A). As the in vitro concentration of NME increases, the

likelihood of cell toxicity may increase. Simultaneous loss of cell viability and reduction in mRNA levels are expected if cell viability alone is the cause; a reduction in mRNA levels without loss of cell viability may indicate downregulation of the DME by the NME.

Prediction of DDI for the Clinical Situation

PK Principles

Organ clearance models are used to estimate intrinsic clearance, as with the following equation:

$$CL = \frac{\left(Q_{\text{organ}} {}^{*} f_u {}^{*} CL_{\text{int}}\right)}{\left(Q_{\text{organ}} + f_u {}^{*} CL_{\text{int}}\right)} \tag{12}$$

where CL is organ clearance, Q is the blood flow to a particular organ, f_u is the fraction unbound in plasma, and CL_{int} is the intrinsic organ clearance of unbound drug (Iwatsubo et al. 1997). High extraction ratio drugs ($Q_{\text{organ}} < < f_u{*}CL_{\text{int}}$) exhibit clearance that is independent of f_u.

$$CL \cong Q_{\text{organ}} \tag{13}$$

Low extraction ratio drugs ($Q_{\text{organ}} > > f_u{*}CL_{\text{int}}$) are dependent upon both the f_u and the intrinsic clearance for activity.

$$CL \cong f_u {}^{*} CL_{\text{int}} \tag{14}$$

For orally dosed drugs, exposure is defined as the area under the plasma concentration-time curve (AUC).

$$AUC_{\text{oral}} = \frac{(F {}^{*} \text{Dose})}{Cl} \tag{15}$$

where bioavailability (F) is defined as

$$F = Fa {}^{*} Fg {}^{*} Fh \tag{16}$$

F_a is the fraction of drug absorbed through the gut wall, F_g is the fraction of drug that escapes the intestine unchanged, and F_h is the amount of drug that escapes from the liver unchanged. For oral drugs eliminated primarily by the liver, the Eqs. 15 and 16 can be combined such that

$$AUC_{\text{oral}} = \frac{(Fa {}^{*} Fg {}^{*} \text{Dose})}{fu {}^{*} CL_{\text{int}}} \tag{17}$$

This equation holds true for both high and low extraction ratio drugs (Benet and Hoener 2002).

Quantitative Prediction of Clinical DDIs

Equations for the reversible inhibition situation already been introduced. Under conditions observed in the clinic, often the concentration of substrate is much lower than the apparent K_m, such that

$$CL_{\text{int}} = \frac{\nu}{[S]} = \frac{V_{\max}}{K_m} \tag{18}$$

For situations with competitive inhibition, the following equation applies:

$$CL_{\text{int},I} = \frac{V_{\max}}{K_m\left(1 + \frac{[I]}{K_i}\right)} \tag{19}$$

Eqs. 18 and 19 can be combined to estimate a change in intrinsic clearance in the inhibited and uninhibited state:

$$\frac{CL_{\text{int}}}{CL_{\text{int},I}} = 1 + \frac{[I]}{K_i} \tag{20}$$

Converting this to a ratio of the area under the plasma-concentration time curves results in the equation

$$AUCR = \frac{AUC_i}{AUC} = 1 + \frac{[I]}{K_i} \tag{21}$$

For drugs with more than one pathway of clearance, Eq. 12 can be rewritten as

$$CL_{\text{int}} = \frac{V_{\max,1}}{K_{m,1}} + \frac{V_{\max,2}}{K_{m,2}} = fm_1{}^{*}CL\text{int} + (1 - fm_1) * CL_{\text{int}} \quad (22)$$

where f_m is the fraction metabolized by a specific pathway (Ito 2005). If only one pathway is inhibited, then

$$CL_{\text{int},I} = \frac{V_{\max,1}}{K_{m,1}\left(1 + \frac{[I]}{K_i}\right)} + \frac{V_{\max,2}}{K_{m,2}} = \frac{fm_1{}^{*}CL_{\text{int}}}{1 + \frac{[I]}{K_i}} + (1 - fm_1) * CL_{\text{int}} \quad (23)$$

To obtain a ratio in the uninhibited and inhibited state, this becomes

$$\frac{CL_{\text{int},I}}{CL_{\text{int}}} = \frac{fm_1}{1 + [I]/Ki} + (1 - fm_1) \quad (24)$$

Equation 24 can be converted from intrinsic clearance to AUC ratio to give

$$AUCR = \frac{1}{\frac{fm_1}{1 + [I]/K_i} + (1 - fm_1)} \quad (25)$$

Equation 25 summarizes the key drivers to observed inhibition in the clinic. The magnitude of DDI effect is dependent upon characteristics of both the perpetrator and victim. For the victim drug, the fraction metabolized (f_m) by the inhibited pathway is a key driver of the magnitude of the DDI effect; the higher the f_m, the larger the potential magnitude of the DDI (Fig. 8). Key features of the perpetrator include the inhibition potency for the particular DME, the unbound fraction, and the free concentration of the inhibitor at the site of inhibition.

Regulatory Guidance and DDIs

Both the EMA and FDA Guidance propose a tiered approach for DDI prediction using basic models, mechanistic static models, and then complex models such as physiologically based pharmacokinetic modeling (PBPK). For basic models, a decision tree scheme for inhibition in line with FDA and EMA Regulatory Guidance is shown in Fig. 9. For reversible inhibition, the following equation holds:

$$AUCR = 1 + [I]/K_i \quad (26)$$

where $AUCR$ is the AUC ratio in the presence and absence of an inhibitor and the inhibitor concentration [I] is the unbound C_{max} value for liver-based DDIs or is calculated using the relationship of dose/250 mL for gut-based DDIs. Exceeding recommended cutoff values ($AUCR$ >1.02 for liver-based DDI and AUCR > 11 for gut-based DDIs) triggers a potential clinically relevant DDI result and a move down the decision tree to more complex mechanistic static models (MSM) or PBPK.

A similar decision tree for TDI is also shown in Fig. 9; the following equation is used to estimate DDI risk, where K_{deg} is the degradation rate of the enzyme of interest. The same [I] definitions apply for this equation as for reversible inhibition, but the cutoff is $AUCR \geq 1.25$.

$$AUCR = \frac{\left(k_{obs} + K_{\text{deg}}\right)}{K_{\text{deg}}} \quad (27)$$

For induction, a decision tree in line with the FDA and EMA DDI Guidance in shown in Fig. 10. The following equation applies, where $AUCR$ is the AUC ratio in the presence and absence of an inducer. In this instance, $AUCR$ <0.8 triggers moving to the next step of the decision tree:

$$AUCR = \frac{1/(1 + dose * E_{\max}{}^{*}[I])}{(EC_{50} + [I])} \quad (28)$$

If a DDI is deemed possible by the basic models, the next step is to assess DDI risk through MSM or dynamic models, especially PBPK. While MSMs incorporate the unbound fraction in plasma to become closer to physiological

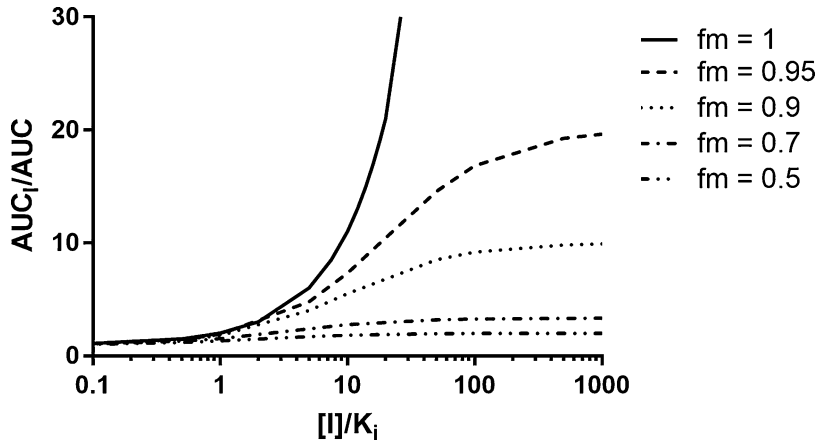

Fig. 8 Impact of f_m and inhibition potency on expected DDI magnitude

relevance, the inhibitor concentration is assumed to be constant and maximal throughout the dose interval. This is a conservative assumption that may not accurately represent the clinical situation for many drugs. Estimation of the overall DDI magnitude is accomplished using Eq. 29 below, which integrates both the expected gut and liver contributions to DDI, as well as the potential contribution of inhibition, inactivation and induction.

$$AUCR = \left(\frac{1}{\mathrm{Inhib}_g{}^{*}\mathrm{Inact}_g{}^{*}\mathrm{Induct}_g{}^{*}\left(1-F_g\right)+F_g}\right) \times * \left(\frac{1}{\mathrm{Inhib}_h{}^{*}\mathrm{Inact}_h{}^{*}\mathrm{Induct}_h{}^{*}fm+(1-fm)}\right) \quad (29)$$

The equations for inhibition ($\mathrm{Inhib}_{\mathrm{organ}}$), inactivation ($\mathrm{Inact}_{\mathrm{organ}}$), and induction ($\mathrm{Induct}_{\mathrm{organ}}$) are shown below, respectively:

$$\mathrm{Inhib}_{\mathrm{organ}} = \frac{1}{1+\frac{[I]_{\mathrm{organ}}}{K_i}} \quad (30)$$

$$\mathrm{Inactiv}_{\mathrm{organ}} \frac{K_{\mathrm{deg,\,organ}}}{K_{\mathrm{deg,\,organ}} + \frac{[I]_{\mathrm{organ}} * k_{\mathrm{inact}}}{[I]_{\mathrm{organ}} + K_I}} \quad (31)$$

$$\mathrm{Induct}_{\mathrm{organ}} = 1 + \frac{\mathrm{dose} * E_{\max}{}^{*}[I]_{\mathrm{organ}}}{\left(EC_{50} + [I]_{\mathrm{organ}}\right)} \quad (32)$$

The concentrations in the gut and liver are defined by the following equations, where $[\mathrm{I}]_{\mathrm{max,\,b}}$ is the maximum concentration of the inhibitor in blood.

$$[I]_{\mathrm{gut}} = \frac{Fa^{*}ka^{*}\mathrm{Dose}}{Q_{\mathrm{enterocyte}}} \quad (33)$$

$$[I]_{\mathrm{liver}} = fu, b^{*}\left([I]_{\max, b} + \frac{Fa^{*}ka^{*}\mathrm{Dose}}{Q_{\mathrm{liver}}}\right) \quad (34)$$

An additional option is PBPK modeling. PBPK is a modeling technology that has seen recent emergence both for internal decision-making for compound progression through drug discovery and development and for regulatory applications (Jamei et al. 2009). PBPK models have three main types of input parameters: demographic and genetic information (i.e., age or gender), physiological information (i.e., organ blood flow and enzyme levels), and drug-specific parameters (i.e., pKa, logP, solubility). Differential equations and Monte Carlo-based simulations integrate the inputs together to simulate a variety of outcomes, including plasma concentration-time profiles, enzyme activity profiles, and drug-tissue concentrations. Because of the types of inputs and the modeling technique used, PBPK is well-suited for modeling where changes in

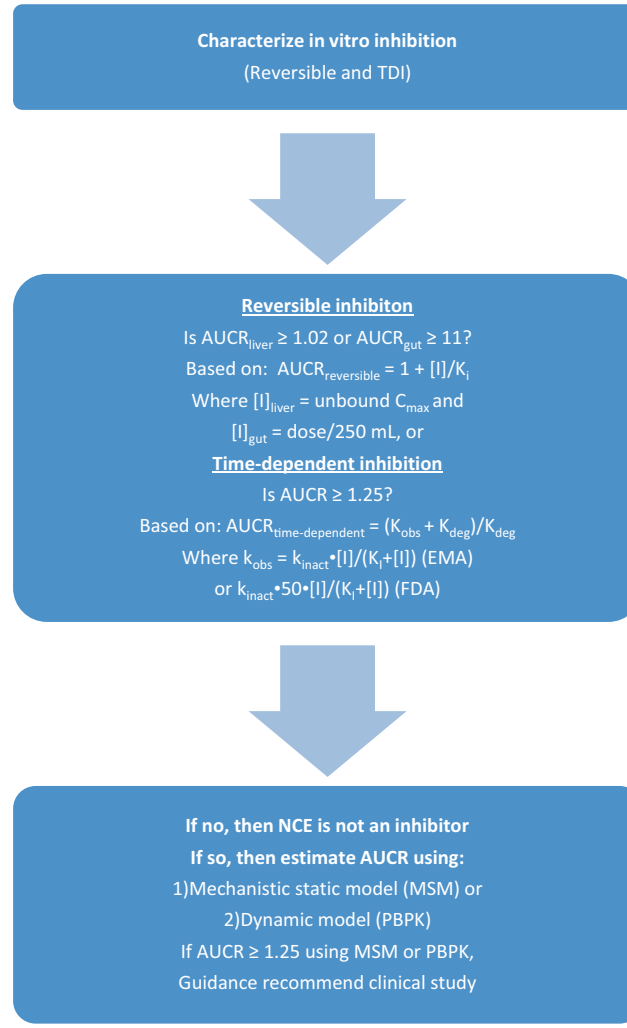

Fig. 9 Basic model decision tree for inhibitory DDIs

physiology or populations may impact PK, changes in physicochemical properties or formulations may impact PK, or where dynamic simulations such as DDIs are desired. PBPK may be used to answer fundamental clinical pharmacology based questions such as (1) what are the intrinsic factors that may influence exposure, (2) what are the extrinsic factors that may influence exposure, and (3) what are situations in which dosing may need to be adjusted due to intrinsic and extrinsic factors. Because physiologically relevant parameters are included, PBPK may more closely represent the clinical situation than basic or MSM models. PBPK may also provide information on expected variability in studies based on demographic factors.

The potency of an inhibitor or inducer is determined based on the magnitude of its interaction with a sensitive probe substrate for a specific enzyme pathway. Strong inhibitors increase AUC $\geq$ fivefold, moderate inhibitors increase AUC two- $\geq$ to $<$ fivefold, and weak inhibitors increase AUC $\geq$ 1.25- to $<$ twofold. Strong inducers reduce AUC $\geq$ 80%, moderate inducers reduce AUC by $\geq$50 to $<$80%, and weak inducers reduce AUC by $\geq$20 to $<$50%.

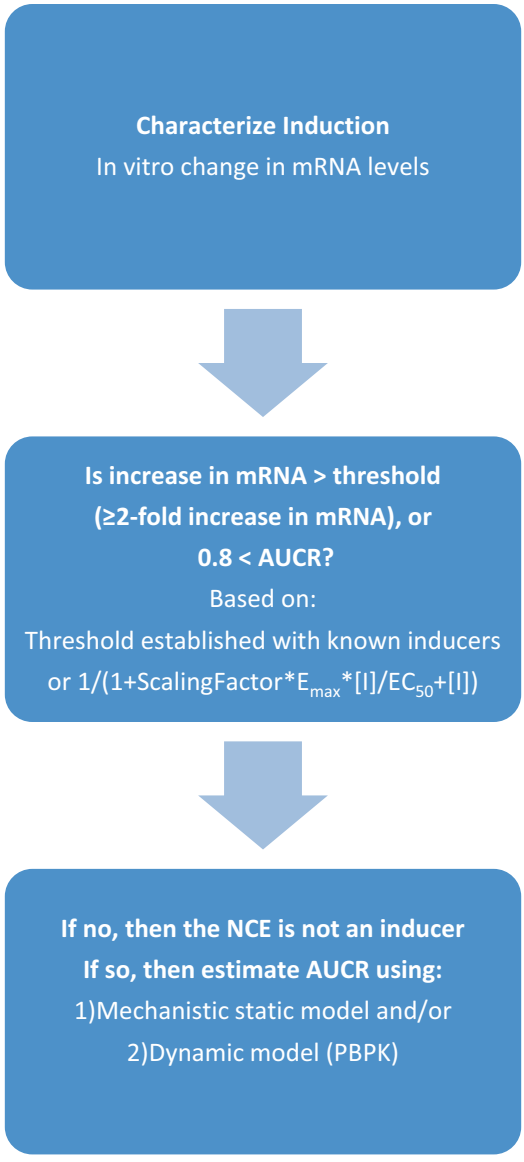

Fig. 10 Basic model decision tree for induction-based DDIs

Additional Considerations

Free Drug Hypothesis

The free drug hypothesis is a tenet of drug discovery and development, which has two fundamental premises (Smith et al. 2010) First, at steady state, drug concentration on either side of a biological membrane is the same. Second, it is free drug at the site of action that is pharmacologically active. While these two proposals may often be true, there are a numbers of situations where the free drug hypothesis may fail. The first premise may fail when drug permeability is low, when uptake transporters increase the concentration of a drug in a tissue, when efflux transporters decrease the concentration of drug in a tissue, or when low or disrupted blood flow may reduce the concentration of drug throughout a tissue. The second premise of the free drug hypothesis may fail when an irreversible inhibitor is involved, when a series of target-mediated events must occur in a series in order to elicit a pharmacological effect, or when in vitro conditions poorly represent the in vivo condition.

These concepts may be more specifically applied to DDIs. Low permeability or efflux of an NME out of the primary organ of clearance, such as the liver, may reduce the magnitude of a DDI. This is rarely observed, as leakiness often provides an alternate mechanism for tissue distribution of a drug. Conversely, uptake of an NME into a primary organ of clearance, such as the liver, may produce a DDI of unexpected magnitude. The concept of in vivo K_i, or $K_{i,iv}$, was developed to help substantiate these observations (Kunze and Trager 1996). $K_{i,iv}$ is a derived parameter shown in Eq. 35 below.

$$\frac{Cl_{\text{int}}}{Cl_{\text{int},I}} = 1 + \frac{[I]}{K_{i,iv}} \tag{35}$$

In an idealized situation, the ratio of in vitro K_i to $K_{i,iv}$ should equal one. Marked deviation from unity indicates the presence of a situation not accounted for in the in vitro experiment, such as mechanism(s) other than reversible inhibition, an active site environment in the in vivo situation that differs from the in vitro conditions, or active uptake or efflux that has altered the relative concentration of perpetrator drug at the enzyme active site. This type of phenomena has been observed clinically for drugs such as fluvoxamine, which has a high liver to plasma partition ratio. Using (S)-mephenytoin as a probe substrate for CYP2C19 activity, the unbound $K_{i,iv}$ was estimated to be 1.9 nM, compared to an unbound

in vitro K_i of 76 nM, a nearly 40-fold increase in estimated inhibition potency in vivo (Yao et al. 2003). Similarly, the $K_{i,iv}$ for the fluvoxamine for its interaction with theophylline (CYP1A2) was estimated at 3.6 nM, while the in vitro K_i was determined to be 36 nM. Conversely, the interaction of the reversible inhibitor fluconazole with the CYP2C9 substrate (S)-warfarin has an estimated $K_{i,iv}$ of 19.8 μM, similar to the measured in vitro K_i of 8 μM, indicating similarity between the in vitro and in vivo environments (Neal et al. 2003).

Is Concern over Plasma Protein Displacement DDIs Justified?

A common misconception is that plasma protein displacement is a major cause of drug interactions. Several early instances of DDI, initially believed to be caused by plasma protein displacement, were later proven to be based on metabolic DDIs. This is understandable based on theoretical considerations, as displacement of a drug from plasma proteins, if occurring, would be compensated for by an increase in intrinsic clearance as more free drug would be available for metabolism; the system would quickly revert back to equilibrium conditions. In a derivation by Benet and Hoener (2002), conversion of Eq. 17 into unbound drug concentration generates the following relationship:

$$AUC_{u,\text{oral}} = f_u{}^{*} AUC_{\text{oral}} = \frac{(Fa^{*}Fg^{*}\text{Dose})}{CL_{\text{int}}} \quad (36)$$

As can be seen, f_u is not involved in the final equation, and thus, changes in f_u are not expected to impact orally administered drugs cleared by the liver. Two unlikely instances where plasma protein displacement could conceivably play a role in DDIs are cases where a narrow therapeutic index drug is dosed intravenously and exhibits a high extraction ratio or where a narrow therapeutic index drug is dosed orally and exhibits a very fast PK/PD equilibrium (Benet and Hoener 2002).

Impact of Pharmacogenetics on DDIs

Pharmacogenetics is the study of how genetic factors impact drug response, where drug selection and dose may be altered depending upon the patient's genetic makeup. Genetic variation in genes expressing DMEs, called polymorphisms, may influence PK. Allelic variants of DMEs may be inactive or have gain or loss of function; the alteration in activity may also be substrate dependent. CYP2C9 is a well-known example, where CYP2C9*1 (wild type), CYP2C9*2, and CYP2C9*3 are the most common allelic variants. Expressed CYP2C9.1, CYP2C9.2, and CYP2C9.3 variants exhibit wild type, reduced, and markedly reduced activity in vitro, respectively (Rodrigues and Rushmore 2002). These CYP2C9 variants also exhibit differing inhibition potency when compared using the same inhibitors (Kumar et al. 2006b) The correlation of genotype to phenotype may be examined using a selective probe substrate of an enzyme. The four types of phenotypes commonly observed are extensive metabolizers (EMs) with typical activity, poor metabolizers (PMs) with no activity due to lack of enzyme expression or expression of inactive enzyme, intermediate metabolizers (IMs) with reduced activity due to one deficient allele, and ultra-rapid metabolizers (UMs) from gain of function variants, including copy number variants (Zanger and Schwab 2013). Examples of DMEs with clinically relevant genetic variation include CYP2C9 (phenytoin and S-warfarin), CYP2D6 (antidepressants and tamoxifen), CYP2C19 (proton pump inhibitors, S-mephenytoin, clopidogrel, and ticlopidine), UGT1A1 (bilirubin, SN-38), and NAT2 (isoniazid, procainamide, and hydralazine). As with DDI, both FDA (Guidance for Industry 2013) and EMA (guideline on key aspects for the use of pharmacogenomics in the pharmacovigilance of medicinal products) have regulatory guidance outlining the assessment of the impact of genotype and phenotype on PK and drug dosing. PK results with differing phenotypes can aid in establishing f_m for that drug using the following equation (Bohnert et al. 2016).

$$fm = 1 - \frac{AUC(EM)}{AUC(PM)} \quad (37)$$

Phenotype may have a marked role in DDIs in certain circumstances, particularly when the main route of clearance is due to a polymorphically expressed enzyme. If, for example, a NCE is primarily cleared by CYP2D6, secondary DMEs may take on the primary role in clearance for CYP2D6 PMs. Co-administration of a drug that inhibits the secondary pathway would normally have minimal effect on the NCE clearance for a CYP2D6 EM but may exhibit a marked DDI effect for the CYP2D6 PM. In vitro characterization of routes of clearance and phenotype assessment of patient characteristics can be pivotal for informing and preventing these types of DDIs.

Conclusion

The theory and practice of understanding and providing quantitative estimates for metabolism-based DDIs has advanced dramatically. In vitro assay design and screening provide information on chemotypes that likely exhibit DDIs in the clinical situation and provide medicinal chemists with the basis to minimize DDI impact through the development of structure-activity relationships early in the discovery process. With the advent of technologies like PBPK, drug metabolism and clinical pharmacology scientists may quantitatively predict the clinical effects of DDIs based on high-content in vitro experiments, even for complex situations where inhibition, inactivation, and induction are all expected simultaneously or where multiple drug entities such as drug metabolites are present. Current frontiers in the field include the prediction of DDIs based on drug metabolism-transporter interplay and the prediction of DDIs for special populations including pediatrics and specific disease states. Understanding of the DDI potential for a clinical drug candidate is gained through the careful generation, examination, and integration of in vitro, preclinical, and clinical data to form a cohesive picture of the absorption, distribution, metabolism, and excretion (ADME) characteristics for that drug.

References and Further Reading

Benet LZ, Hoener BA (2002) Changes in plasma protein binding have little clinical relevance. Clin Pharmacol Ther 71:115–121

Bjornsson TD, Callaghan JT, Einolf HJ, Fisher V, Gan L, Grimm S, Kao J, King SP, Miwa G, Ni L, Kumar G, McLeod J, Obach SR, Roberts S, Roe A, Shah A, Snikeris F, Sullivan JT, Tweedie D, Vega JM, Walsh J, Wrighton SA (2003) The conduct of in vitro and in vivo drug-drug interaction studies: a PhRMA perspective. J Clin Pharmacol 43:443–469

Bohnert T, Patel A, Templeton I, Chen Y, Lu C, Lai G, Leung L, Tse S, Einolf H, Wang Y-H, Sinz M, Stearns R, Walsky R, Geng W, Sudsakorn S, Moore D, He L, Wahlstrom J, Keims J, Narayanan R, Lang D, Yang Q (2016) Evaluation of a new molecular entity as a victim of metabolic drug-drug interactions – an industry perspective. Drug Metab Dispos 44:1399–1423

Chu V, Einolf HJ, Evers R, Kumar G, Moore D, Ripp S, Silva J, Sinha V, Sinz M, Skerjanec A (2009) In vitro and in vivo induction of cytochrome P450: a survey of the current practices and recommendations: a pharmaceutical research and manufacturers of America perspective. Drug Metab Dispos 37:1339–1354

Chung J, Alvarez-Nunez F, Chow V, Daurio D, David J, Dodds M, Emery M, Litweiler K, Paccaly A, Peng J, Rock B, Wienkers L, Yang C, Yu Z, Wahlstrom J (2015) Utilizing physiologically based pharmacokinetic modeling to inform formulation and clinical development for a compound with pH-dependent solubility. J Pharm Sci 104:1522–1532

Day RO, Snowden L, McLachlan AJ (2017) Life-threatening drug interactions: what the physician needs to know. Intern Med J 47:501–512

Dickmann LJ, Patel SK, Rock DA, Wienkers LC, Slatter JG (2011) Effects of interleukin-6 (IL-6) and an anti-IL-6 monoclonal antibody on drug-metabolizing enzymes in human hepatocyte culture. Drug Metab Dispos 39:1415–1422

European Medicine Agency (EMA), Committee for Human Medical Products (CHMP) (2012) Guideline on the investigation of drug interactions. http://www.ema.europa.eu/docs/en_GB/document_library/Scientific_guideline/2012/07/WC500129606.pdf

European Medicine Agency (EMA), Committee for Human Medical Products (CHMP) (2015) Guideline on key aspects for the use of pharmacogenomics in the pharmacovigilance of medicinal products. http://www.ema.europa.eu/docs/en_GB/document_library/Scientific_guideline/2015/11/WC500196800.pdf

Evers R, Dallas S, Dickmann LJ, Fahmi OA, Kenney JR, Kraynov E, Nguyen T, Patel AH, Slatter JG, Zhang L

(2013) Critical review of preclinical approaches to investigate cytochrome P450-mediated therapeutic protein drug-drug interactions and recommendations for best practices: a white paper. Drug Metab Dispos 41:1593–1609

FDA Guidance for Industry (2013) Clinical pharmacogenomics: premarket evaluation in early-phase clinical studies and recommendations for labeling. https://www.fda.gov/downloads/Drugs/GuidanceComplianceRegulatoryInformation/Guidances/UCM337169.pdf

FDA Guidance for Industry (2017a) Clinical drug interaction studies – study design, data analysis, and clinical implications. https://www.fda.gov/downloads/Drugs/GuidanceComplianceRegulatoryInformation/Guidances/UCM292362.pdf

FDA Guidance for Industry (2017b) In vitro metabolism and transporter-mediated drug-drug interaction studies. https://www.fda.gov/downloads/drugs/guidancecomplianceregulatoryinformation/guidances/ucm581965.pdf

Foti RS, Rock DA, Wienkers LC, Wahlstrom JL (2010) Selection of alternative CYP3A4 probe substrates for clinical drug interaction studies using in vitro data and in vivo simulation. Drug Metab Dispos 38:981–987

Foti RS, Rock DA, Pearson JT, Wahlstrom JL, Wienkers LC (2011) Mechanism-based inactivation of cytochrome P450 3A4 by mibefradil through heme destruction. Drug Metab Dispos 39:1188–1195

Frere J-M, Leyh B, Renard A (1983) Lineweaver-Burk, Hanes, Eadie-Hofstee and Dixon plots in non-steady-state situations. J Theor Biol 101:387–400

Grimm SW, Einolf HJ, Hall SD, He K, Lim HK, Ling KH, Lu C, Nomeir AA, Seibert E, Skordos KW, Tonn GR, VanHorn R, Wang RW, Wong YN, Yang TJ (2009) The conduct of in vitro studies to address time-dependent inhibition of drug-metabolizing enzymes: a perspective of the pharmaceutical research and manufacturers of America. Drug Metab Dispos 37:1355–1370

Hutzler JM, Tracy TS (2002) Atypical kinetic profiles in drug metabolism reactions. Drug Metab Dispos 30:355–362

Ito K, Hallifax D, Obach RS, Houston JB (2005) Impact of parallel pathways of drug elimination and multiple cytochrome P450 involvement on drug-drug interactions: CYP2D6 paradigm. Drug Metab Dispos 33:837–844

Iwatsubo T, Hirota N, Ooie T, Suzuki H, Shimada N, Chiba K, Ishizaki T, Green CE, Tyson CA, Sugiyama Y (1997) Prediction of in vivo drug metabolism in the human liver from in vitro metabolism data. Pharmacol Ther 73:147–171

Jacubeit T, Drisch D, Weber E (1990) Risk factors as reflected by an intensive drug monitoring system. Agents Actions 29:117–125

Jamei M, Marciniak S, Feng K, Barnett A, Tucker G, Rostami-Hodjegan A (2009) The Simcyp population-based ADME simulator. Expert Opin Drug Metab Toxicol 5:211–223

Korzekwa KR, Krishnamachary N, Shou M, Ogai A, Parise RA, Rettie AE, Gonzales FJ, Tracy TS (1998) Evaluation of atypical cytochrome P450 kinetics with two-substrate models: evidence that multiple substrates can simultaneously bind to cytochrome P450 active site. Biochemistry 37:4137–4147

Kumar V, Locuson CW, Sham YY, Tracy TS (2006a) Amiodarone analog-dependent effects on CYP2C9-mediated metabolism and kinetic profiles. Drug Metab Dispos 34:1688–1696

Kumar V, Wahlstrom JL, Rock DA, Warren CJ, Gorman LA, Tracy TS (2006b) CYP2C9 inhibition: impact of probe substrate selection and pharmacogenetics on in vitro inhibition profiles. Drug Metab Dispos 34:1966–1975

Kunze KL, Trager WF (1993) Isoform-selective mechanism-based inhibition of cytochrome P450 1A2 by furafylline. Chem Res Toxicol 6:649–656

Kunze KL, Trager WF (1996) A rational approach to management of a metabolically based drug interaction. Drug Metab Dispos 24:429–435

Levy G (1998) What are narrow therapeutic index drugs? Clin Pharmacol Ther 63:501–505

Lin JH (2006) CYP induction-mediated drug interactions: in vitro assessment and clinical implications. Pharm Res 23:1089–1116

Lin JH, Lu AYH (1997) Role of pharmacokinetics and metabolism in drug discovery and development. Pharmacol Rev 49:403–449

Lin Y, Lu P, Tang C, Mei Q, Sandig G, Rodrigues AD, Rushmore TH, Shou M (2001) Substrate inhibition kinetics for cytochrome P450-catalyzed reactions. Drug Metab Dispos 29:368–374

Lineweaver H, Burk D (1934) The determination of enzyme dissociation constants. J Am Chem Soc 56:658–666

Michaelis L, Menten ML (1913) Die kinetic der invertinwirkung. Biochem Z 49:333–369

Neal JM, Kunze KL, Levy RH, O'Reilly RA, Trager WF (2003) Kiiv, an in vivo parameter for predicting the magnitude of a drug interaction arising from competitive enzyme inhibition. Drug Metab Dispos 31:1043–1048

Rodrigues AD, Rushmore TH (2002) Cytochrome P450 pharmacogenetics in drug development: in vitro studies and clinical consequences. Curr Drug Metab 3:289–309

Rowland M, Martin SB (1973) Kinetics of drug-drug interactions. J Pharmacokinet Biopharm 1:553–567

Silverman RB (1995) Mechanism-based inactivators. Methods Enzymol 249:240–283

Smith DA, Di L, Kers EH (2010) The effect of plasma protein binding on in vivo efficacy: misconceptions in drug discovery. Nat Rev Drug Discov 9:929–929

VandenBrink BM, Foti RS, Rock DA, Wienkers LC, Wahlstrom JL (2012) Prediction of CYP2D6 drug interactions from in vitro data: evidence for substrate-dependent inhibition. Drug Metab Dispos 40:47–53

Wahlstrom JL, Rock DA, Slatter JG, Wienkers LC (2006) Advances in predicting CYP-mediated drug

interactions in the drug discovery setting. Expert Opin Drug Discov 1:677–691

Wienkers LC, Heath TG (2005) Predicting in vivo drug interactions from in vitro drug discovery data. Nat Rev Drug Discov 4:825–833

Yao C, Kunze KL, Kharasch ED, Wang Y, Trager WF, Ragueneau I, Levy RH (2001) Fluvoxamine-theophylline interaction: gap between in vitro and in vivo inhibition constants toward cytochrome P4501A2. Clin Pharmacol Ther 70:415–424

Yao C, Kunze KL, Trager WF, Kharasch ED, Levy RH (2003) Comparison of in vitro and in vivo inhibition potencies of fluvoxamine toward CYP2C19. Drug Metab Dispos 31:565–571

Zanger UM, Schwab M (2013) Cytochrome P450 enzymes in drug metabolism: regulation of gene expression, enzyme activities, and impact of genetic variation. Pharmacol Ther 138:103–141